Remnants of large magnitude earthquakes: Evidences from the Great Rann sediments, Kachchh, Western India

Parag S. Sohoni and Javed N. Malik

Department of Geology, M.S. University of Baroda, Vadodara 390 002, India

During our investigations on the seismicity of the Kachchh region of Gujarat, we recorded a variety of seismically-induced deformational features from the Great Rann sediments. The structures identified, viz. small-scale folding, pseudo-sand blow, sand dike and micro-faulting from the newly-excavated trenches are attributed to liquefaction and fluidization of water-saturated sediment resulting due to upward propagation of cyclic shear waves, generated during earthquake. Other features identified were craters with no connecting feeder dikes from the bottom. We envisage that these craters might have been formed due to sudden down slip along en-echelon faults developed at the crest and on the limb of an anticlinal structure (? Ludiya anticline), suggestive of reactivation of anticlinal structure caused by the tectonic movement during Holocene period. These structures provide not only more data on the diversity of the deformational features, but also enable to suggest the likely tectonic mechanism responsible for the genesis of these structures, and point to the occurence of seismic events of magnitude $M_s \geq 5$ which may have been responsible for the deformation of the Holocene sediments of Rann.

THE Kachchh peninsula has a long history of earthquakes of varying intensities/magnitudes. Many devastating earthquakes have been recorded in the recent historic past[1–6], of which the most remarkable earthquake occurred on 16 June 1819 in the Great Rann of Kachchh (Allah Band) with magnitude M_s 7.8 (ref. 5) and reached maximum intensity of IX to X+(MM) (ref. 4). This earthquake is one of the largest recorded seismic movements in the entire Indian shield[5]. The region is considered to be active since Mesozoic times and movements along the master E–W faults have played a significant role in shaping the present day physiography of Kachchh[7]. Evidences like drainage derangement and recent gully erosion along the margin of Great Rann and Banni plains are suggestive of tectonic movements during Quaternary period[8,9].

From the available earthquake data documented by earlier workers[1–6] and data from Indian Meteorological Department, it appears that the Great Rann and Banni plains are seismically active areas of Kachchh (Table 1). The significance of the present study is to identify the remnants of the large magnitude earthquakes that occurred in this area during Holocene period.

In the course of our investigations on the seismicity and neotectonism of the Kachchh region of western India, we have come across some examples of deformational features like small-scale folding, micro-faulting, pseudo-sand blow, sand dike, pseudo-nodules, intrusive flame structure, sediment plume, contorted laminae and craters with no feeder dikes in the unconsolidated soft sediments of the Great Rann and Banni plains from excavated trench sites 1 and 2 (near Bhirandiyala, 53 km north of Bhuj) and sites 3–7 (near Ludiya, 3 km south of Khavda) (Figure 1). The present studies lay emphasis on trench sites – 3, 4, 5, and 6 (Figure 1).

The purpose of this short research communication is to provide information on the soft sediment deformational structures with a view to substantiate the already existing data on the diversity of the deformational features, and to suggest the likely tectonic mechanism responsible for the genesis of these structures in the Great Rann area. The Rann sediments owe their sedimentation under deltaic/intertidal environments by ancient rivers draining the area from north[10,11]. The originally flat gradientless topography and absence of overburden rules out the possibilities of these structures being influenced by burial-related deformation or by slope failure. Hence, the formation of these deformational structures in the unconsolidated soft sediments could be due to compressional stresses which developed because of seismic shaking as a possible result of earthquakes which visited the Great Rann in the Recent past.

The trench site 3 near Ludiya, shows deformational structures like well-developed small-scale folding, pseudonodules and a feature closely resembling a sand blow (Figure 2). The folding is marked by broad syncline and anticline, without obliterating the primary laminations of clay/silt. This folding does not resemble the crumpling or complicated folding of laminae developed due to penecontemporaneous nonseismic deformation[12]. Thus the formation of this structure can be attributed to intense compressional stresses developed due to seismic shaking[13–17]. Another feature which resembles a sand blow, no associated feeder dike was found, which is not only unlike a typical sand blow, but also shows distinct traces of convolutions. To explain this, it is envisaged that at one of the ends, the presence of clay acted as a barrier against the push, thereby causing the sand-silt lense to form a bulbous bulge which abutts against the massive clays and the junction is marked by a micro-fracture (Figure 2). We have preferred to call this structure a 'pseudo-sand blow'. A good example of sand dike (Figure 3), a typical liquefaction feature has however, been encountered at the trench site 4, 50 m to the south of trench site 3 (Figure 1). The formation of this sand dike is attributed to the cyclic shear stresses, which develop during an earthquake event, causing build up of pore water pressure, which, in turn, leads to liquefaction and fluidization of the water-saturated cohesionless

Table 1. List of earthquakes that visited the Great Rann and its surroundings (1668–1993)

Date	Latitude	Longitude	Location	Mag/Int	Reference
1668	25.00	68.00	Great Rann	7	1
16 Jun. 1819	24.00	70.00	Allah Band	7.8	2
19 Apr. 1845	24.00	69.00	Great Rann	VIII	3
25 Apr. 1845	24.00	69.00	Great Rann	5.5	1
19 Jun. 1845	23.80	68.90	Indus delta	VII	3
29 Apr. 1864	24.00	70.00	Great Rann	6	1
20 Aug. 1888	—	—	Khavda	Slight	4
1 Jun. 1890	—	—	Lakhpat, Khavda	Slight	4
14 Jan. 1903	24.00	70.00	Great Rann	VII	3
30 Jul. 1904	—	—	Khadir	Slight	4
11 Jan. 1905	—	—	Khadir	Slight	4
30 Jun. 1906	—	—	Khavda, Lakhpat	Slight	4
12 Mar. 1907	—	—	Khavda	Slight	4
12 July 1907	—	—	Khavda, Khadir	Slight	4
9 Oct. 1907	—	—	Khavda	Slight	4
29 Sep. 1908	—	—	Khavda	Slight	4
21 Oct. 1908	—	—	Khavda	Slight	4
31 Nov. 1908	—	—	Khadir, Khavda	Slight	4
7 Feb. 1909	—	—	Khavda	Slight	4
1 Aug. 1910	—	—	Khavda	Slight	4
13 Dec. 1910	—	—	Khavda	Slight	4
14 Mar. 1912	—	—	Khadir	Slight	4
1 Oct. 1912	—	—	Khavda	Slight	4
7 Nov. 1912	—	—	Khadir	Slight	4
26 Jun. 1913	—	—	Khavda	Slight	4
21 Feb. 1921	—	—	Khavda, Lakhpat	Slight	4
26 Oct. 1921	25.00	68.00	Indus delta	5.5	1
5 Mar. 1924	—	—	Khavda	Slight	4
18 Nov. 1927	—	—	Khavda, Rapar	Moderate	4
31 Oct. 1940	23.70	69.90	Banni	5.8	1
26 Mar. 1965	24.18	69.56	Indo-Pak border	5	1
27 May. 1965	24.46	68.69	N of Kachchh	5	1
26 Apr. 1981	24.13	69.51	Indo-Pak border	4.1	1
31 Jan. 1982	24.10	69.60	Indo-Pak border	4.8	3
7 Apr. 1985	24.30	69.90	Indo-Pak border	5	3
21 Mar. 1989	24.28	69.00	Indo-Pak border	4	1
10 Sep. 1990	24.17	68.68	Indus delta	4.7	1
9 Feb. 1993	24.60	69.00	N of Kachchh	4.3	1

1. Data obtained from IMD, New Delhi, in the year 1996–97.
2. Johnston and Kanter[5].
3. Quittmeyer and Jacob[4].
4. *Kachchh Gazetteer*, Govt. Press and Stationary Dept, 1971, pp. 56–61.

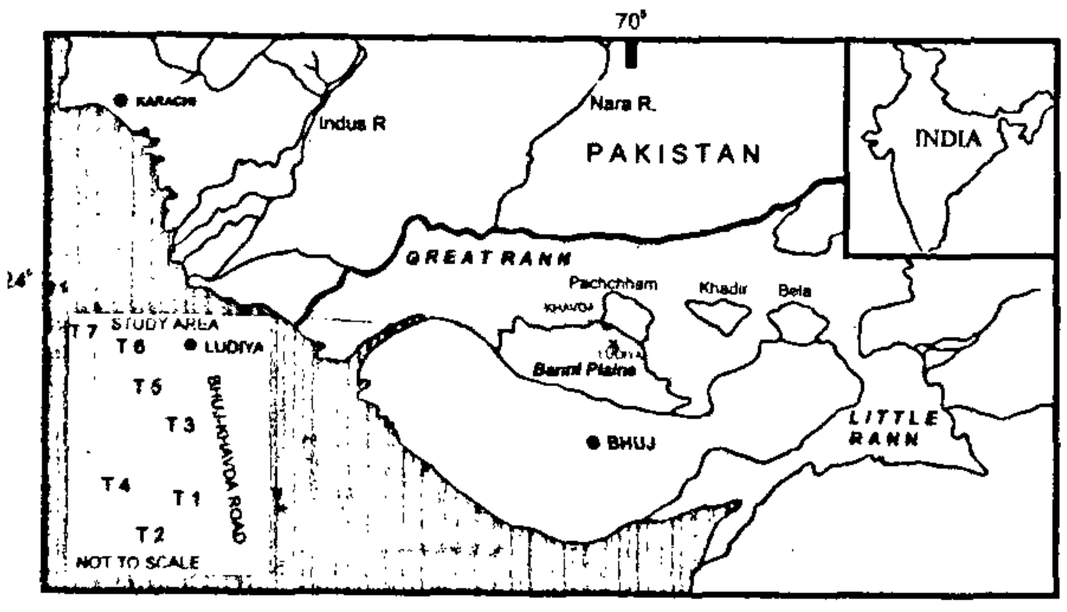

Figure 1. Location of the study area showing the trench sites near Ludiya and Bhirandiyala, in Great Rann and Banni plains.

sediment[17]. Here, the sand shows intrusion and breaking of the overlying comparatively thick clay layer, spreading out on either side of the vent along horizontal parting laminae, without reaching the surface. This suggests that seismic shaking must have lasted for shorter duration and was unable to produce strong hydraulic forces to lead sand venting upto the surface, because the zone of liquefaction during seismic event depends on the intensity and duration of ground motion which generate cyclic shear stresses during an earthquake[17]. Further, the presence of sand dike suggests a seismic event of magnitude ≥ 5 M[17–19]. However, some more occurrences of sand dikes and sand blows would throw light on the possible magnitudes of the event/s.

The trench site 5 shows an example of slumping along almost straight fault plane near the surface and no signatures of curved or concave upward surface were observed (Figure 4 *a*). A clear-cut graben-like feature

Figure 2. Photomosaic of N–S trending trench site 3, showing seismically-induced structures. PSB, pseudo-sand blow; FL, folding of clay/silt laminae; DL, discontinuous laminae; DC, deformed charcoal bed; f, micro-fracture.

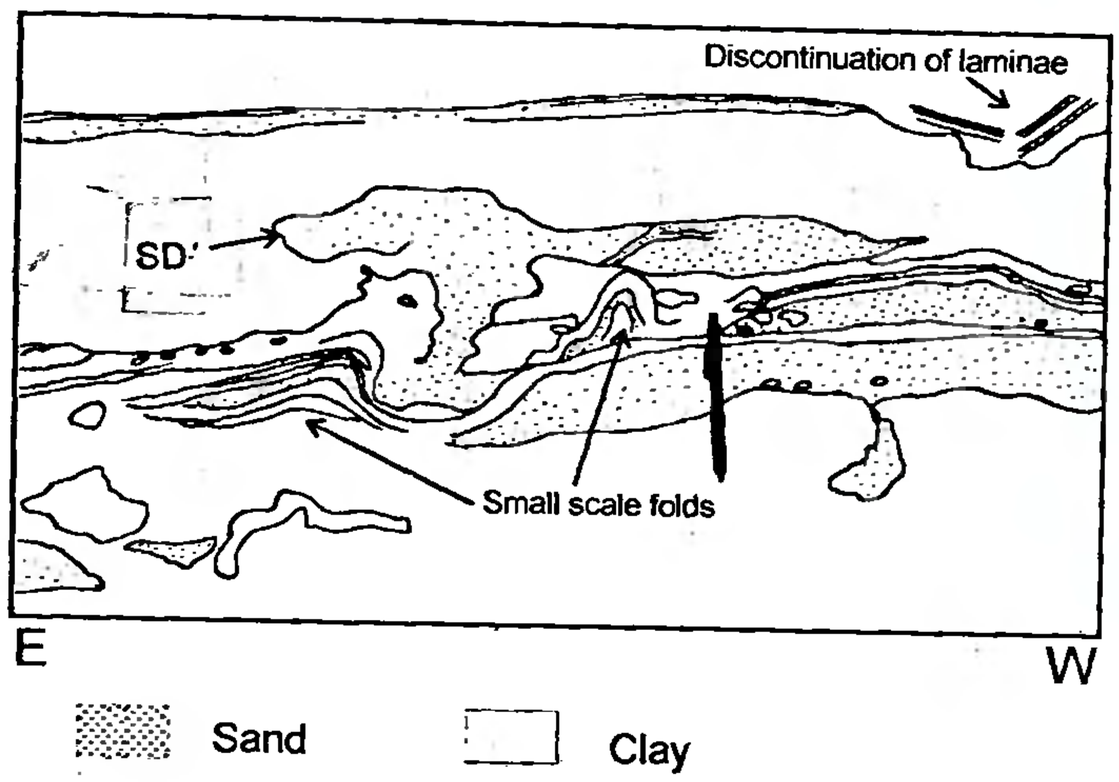

Figure 3. Line drawing of trench site 4 showing SD, sand dike along with small-scale folds (Scale: length of pen is 14 cm).

cutting across the laminated clay and silt is observed at the basal portion of the trench (Figures 4 *a*, *b*). The fault is capped by the laminated clayey-silt and silty-sand horizons, suggesting that the upper horizon was deposited subsequent to faulting under channel-fill deposition. Interestingly, the sediment succession within the channel-fill deposit, comprising fine laminations of clayey-silts and silty-sand, are also seen disturbed-warped and micro-faulted (Figures 4 *a*, *b*). From this, it is envisaged that these deformational features are net result of one single large magnitude earthquake.

At trench site 6, (about 175 m north of trench site 3), we observed well-developed craters (Figure 5 *a*). The craters are not connected with any feeder dikes from the bottom. The formation of these craters are mainly attributed to more or less sub-parallel buried faults, and it is quite possible that the craters represent a depression/graben that developed along the crest and on the limb of an anticline (? Ludiya anticline[20,21]). This probably suggests reactivation of the anticlinal structures during Late Holocene times. Yeats *et al.*[18], have invoked such

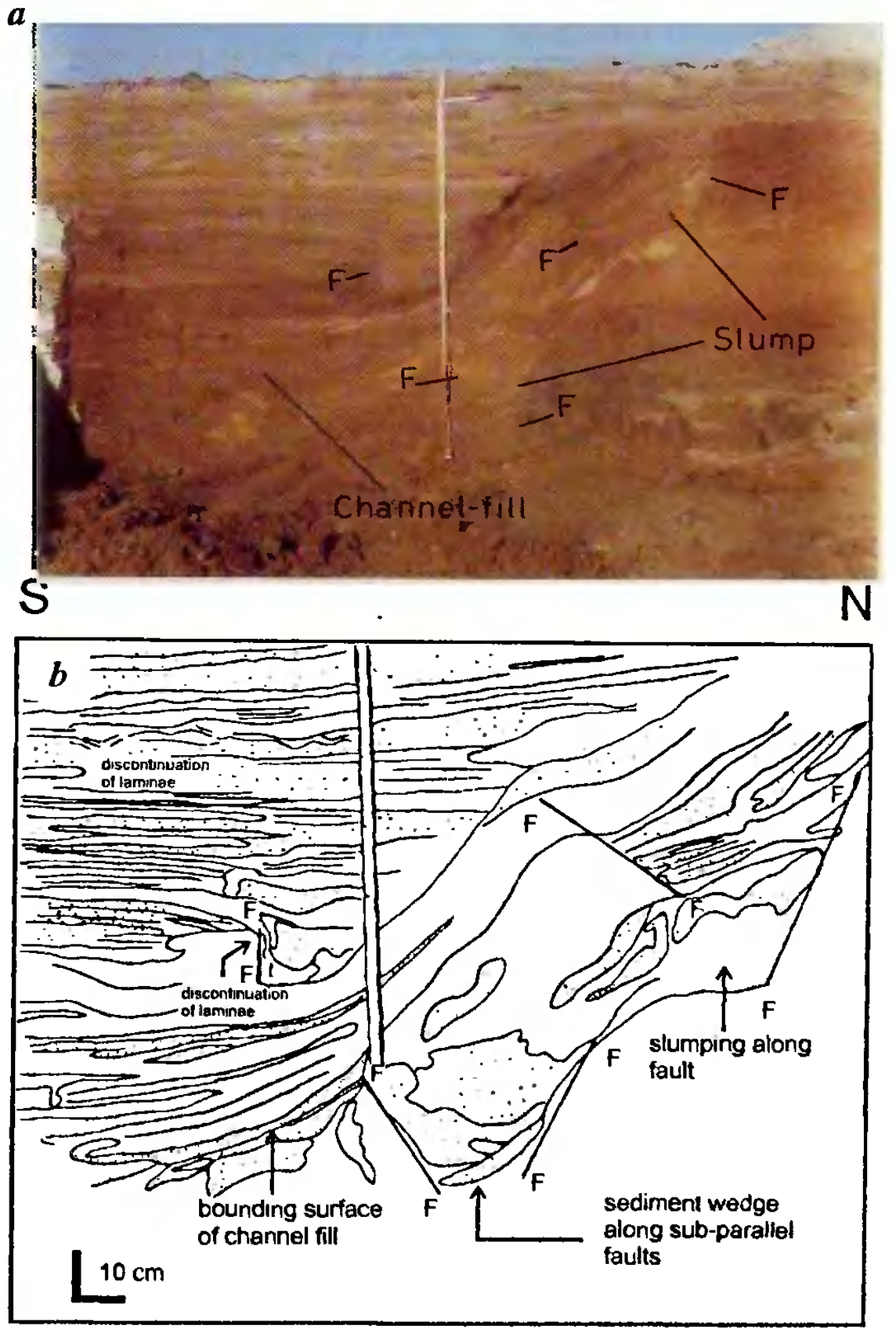

Figure 4. *a*, Photograph of east facing wall of N–S oriented trench site 5, showing deformational structures formed due to a single large event. F, Fault. *b*, Line drawing of trench site 2 showing slumping along almost straight fault plane on the right hand side of the trench and faulting resulting in formation of wedge (in the bottom right) and channel-fill deposits marked by shallow trough showing concave upward bounding surface that scoured the earlier succession subsequent to faulting. Also, the slumping of the sediment and discontinuation of silty-sand and clay laminae is seen within the channel-fill.

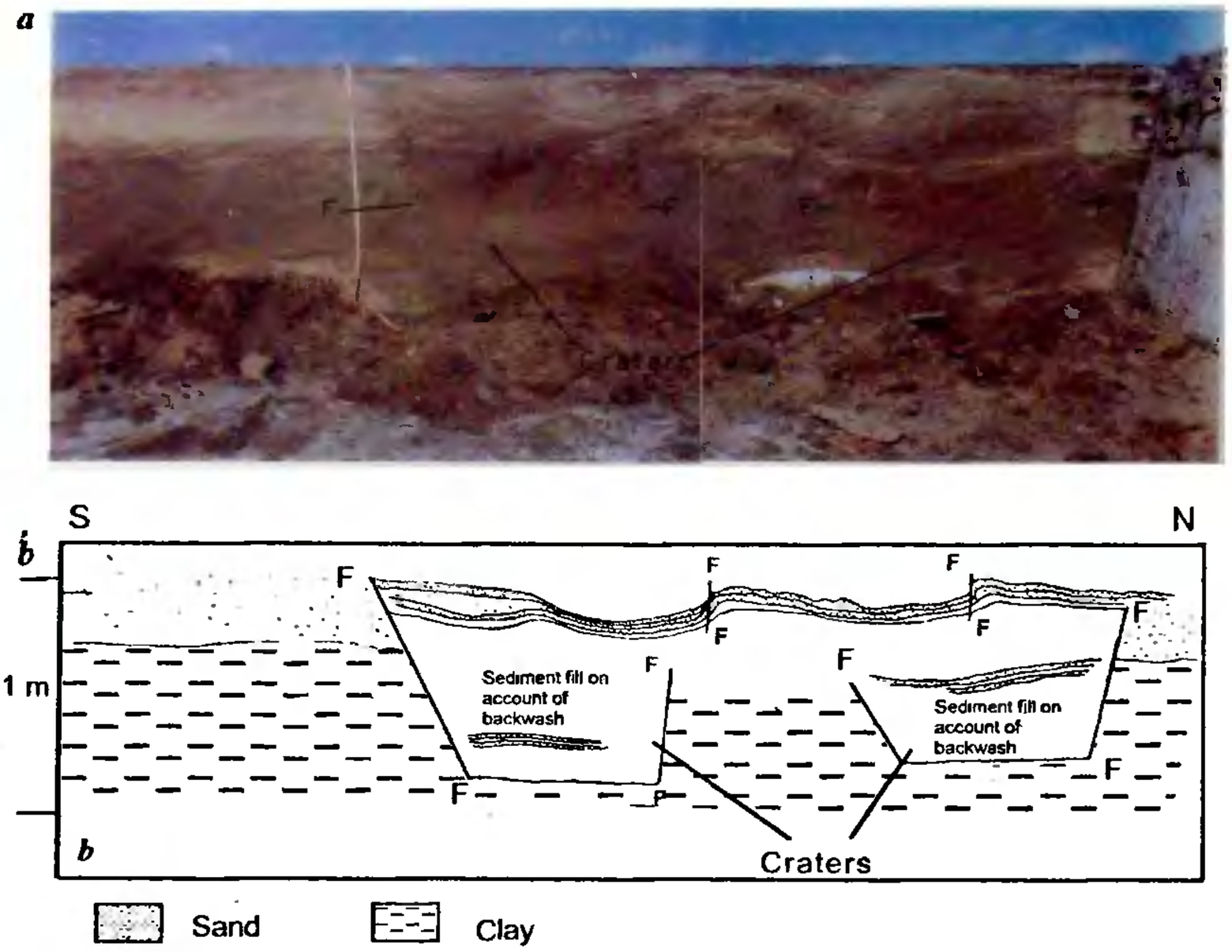

Figure 5. *a*, Photomosaic of N–S oriented trench site 6 showing well-developed craters. *b*, Line drawing showing formation of craters on account of differential slip along en-echelon faults developed at the crest of an anticline and discontinuation of laminae along minor subordinate faults.

a mechanism for the development of crater-like structures with no connecting feeder dikes. In this case a sudden down-slip along the faults at the crest of an anticline, are invoked to have produced high-pore water pressure, thereby causing the sudden evacuation of the material from the core of the fold[18]. The sediment succession within the crater comprise mainly silty-clay and is overlain by a silty sand unit, the deposition of which may be due to the backwash. In this unit also, some small-scale faults are observed (Figure 5 *b*).

The widespread occurrence of deformational features (between Bhirandiyala and Ludiya – 17 km), originally showing flat topography and absence of overburden rules out the possibilities of the structures being influenced by burial-related nonseismic deformation or by slope failure. Thus, the structures identified near Ludiya are interpreted to be of seismic origin. It is highly possible that almost all the structures were formed by a single large magnitude seismic event. The lack of soil development at all the sites indicates that the event must have occurred sometime in Recent past. Although, presence of liquefaction and faulting structures at the four sites near Ludiya are attributed to the single historic earthquake, however precise dates would throw much more light on their occurrence and the related seismic events that caused their formation.

Though, the evidence of structural offset and sand dike is rather inconclusive from the point of view of magnitude estimation, the formation of the seismicity-related structures in the upper portion of the Rann sediments definitely points to these being related to some of the more recent historical earthquakes, of relatively high magnitude.

1. MacMurdo, J., *Philos. Mag.*, 1824, **63**, 105–177.
2. Oldham, T., *Mem. Geol. Surv. India*, 1883, **19**, 163–213.
3. Oldham, R. D., *Mem. Geol. Surv. India*, 1926, **46**, 1–77.
4. Quittmeyer, R. C. and Jacob, K. H., *Bull. Seismol. Soc. Am.*, 1979, **69**, 773–823.
5. Johnston, A. C. and Kanter, L. R., *Sci. Am.*, 1990, 68–75.
6. Gowd, T. N., Srirama Rao, S. V. and Chary, K. B., *Pageoph*, 1996, **146**, 1–27.
7. Biswas, S. K., *Indian J. Earth Sci.*, 1974, **2**, 177–190.
8. Kar, A., in *Geomorphology and Environment* (eds Singh, S. and Tiwari, R. C.), Allahabad Geogr. Soc., Allahabad, 1988, pp. 300–310.
9. Kar, A., *Geomorphology*, 1993, **8**, 199–219.
10. Glennie, K. W. and Evans, G., *Sedimentol.*, 1973, **23**, 625–647.
11. Shrivastava, P. K., *J. Geol. Soc. India*, 1971, **12**, 392–395.
12. Reineck, H. E. and Singh, I. B., *Depositional Sedimentary Environments with Reference to Terrigenous Clastics*, Springer-Verlag, 1980, 2nd edn, p. 542.
13. Sims, J. D., *Science*, 1973, **182**, 161–163.
14. Sims, J. D., *Tectonophysics*, 1975, **29**, 141–152.
15. Lowe, D. R., *Sedimentol.*, 1975, **22**, 157–204.
16. Scott, B. and Price, S., *Tectonophysics*, 1988, **147**, 165–170.
17. Obermeir, S. F., *Eng. Geol.*, 1996, **44**, 1–76.
18. Yeats, R. S., Sieh, K. and Allen, C. R., in *Geology of Earthquakes*, Oxford University Press, 1997, p. 568.

19. Ambrayses, N. N., *Earthquake Eng. Structural Dynamics*, 1988, **17**, 1–105.
20. Biswas, S. K., Proceedings of the Third Indian Geological Congress at Pune, 1980, pp. 255–272.
21. Biswas, S. K., *Tectonophysics*, 1987, **135**, 307–327.

ACKNOWLEDGEMENTS. We are indebted to Prof. S. S. Merh for the guidance and suggestions during the preparation of this manuscript. We are thankful to Dr R. V. Karanth for valuable discussion and constant encouragement. Financial support provided by the Department of Science and Technology, New Delhi (No. DST/23(1)/ESS/95) is also gratefully acknowledged.

Received 24 October 1997; revised accepted 24 March 1998

In situ detection of phytoplasma in spike-disease-affected sandal using DAPI stain

Sunil Thomas and M. Balasundaran

Division of Pathology, Kerala Forest Research Institute, Peechi, Thrissur 680 653, India

Free-hand sections of spike-disease-affected sandal (*Santalum album* L.) and its hosts were stained with the DNA-binding fluorochrome, 4,6,diamidino-2-phenyl indole (DAPI), to detect the presence of phytoplasma. Yellow-green fluorescence was detected in the phloem of diseased sandal. While the phloem tissue of healthy sandal and host plants growing close to the spike-disease-affected sandal in the field as well as in glass house did not show fluorescence. The intensity of fluorescence was high in the young stem and inner bark compared to the root, petiole and leaf. When the efficiency of the DAPI stain was compared with Dienes' stain to detect phytoplasma, the latter was found to be less efficient.

SANDAL (*Santalum album* L.), a semi-root-parasitic tree is known for its highly valuable wood and oil. Spike disease, reported from all the major sandal-growing states of India is the most serious disease of the species. The disease is characterized by extreme reduction in leaf size accompanied by stiffening and reduction of internode length. In advanced stage, the entire shoot gives the appearance of a spike inflorescence. Spiked trees die within two-to-three years after the appearance of visible symptoms[1]. The causative agent of this disease, phytoplasma, a nonculturable plant mycoplasma observed exclusively in the phloem, was first detected in 1969 by electron microscopy[2–4].

Since then, number of staining techniques have been tested to improve the detection of phytoplasma in plants, and to reduce dependency on electron microscope for identification of yellows diseases[5]. Light-microscopic-detection of phytoplasma involves indirect detection, whereby callose formed in sieve elements of phloem tissue as a response to wounding, is visualized by staining with either aniline blue[6,7] or Giemsa stain[8]. Direct detection of phytoplasma in little-leaf-affected eucalyptus was reported by Ghosh *et al.*[9] using Dienes' stain, a mycoplasma-specific stain. A DNA-binding fluorochrome, Hoechst 33258, has been used to detect phytoplasma in spike-disease-affected sandal[7].

The availability of sensitive and selective fluorescent probes for living cells has opened new horizons in cell biology. The fluorescence signal, superimposed against a dark background, permits sharper cytological details to be observed than with a comparable stained specimen

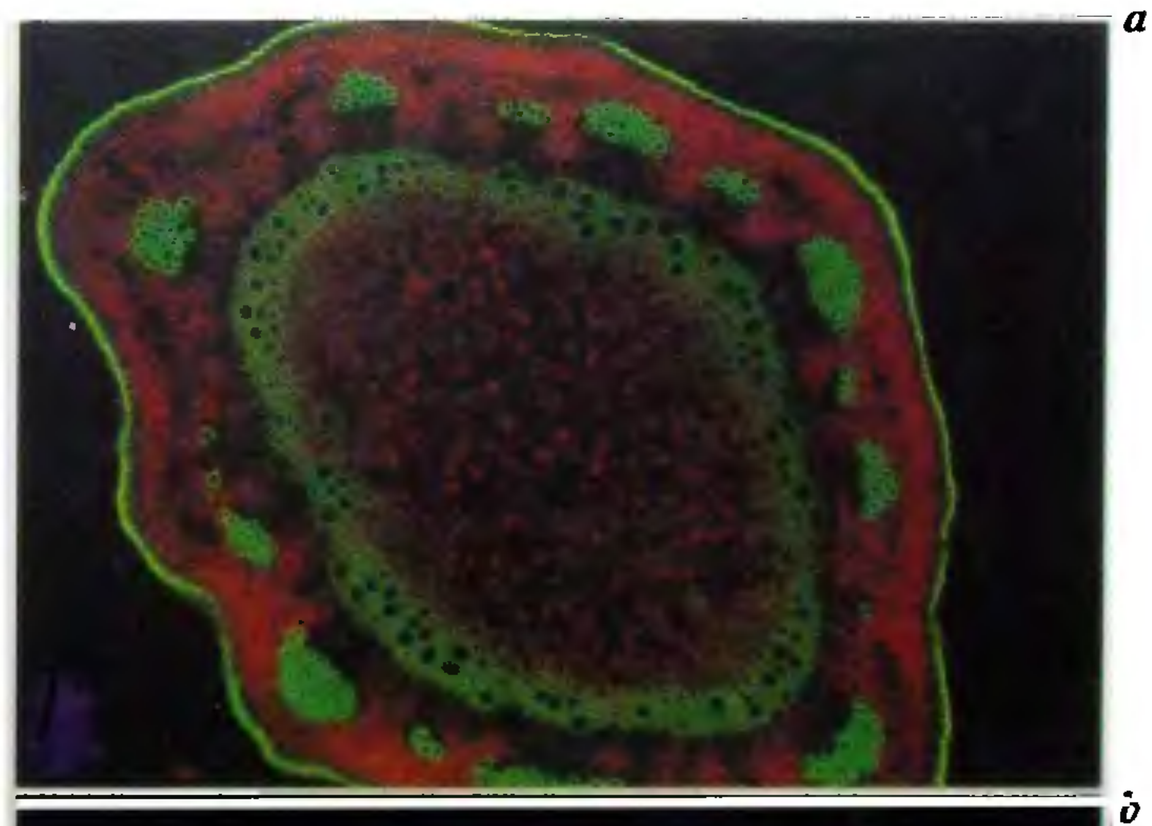

Figure 1. Fluorescent photomicrograph of healthy (*a*) and diseased (*b*) sandal stem (cross section) stained with DAPI (×70). Note the fluorescent spots in the phloem of diseased tissue.